Am J Transl Res 2016;8(4):1838-1847
www.ajtr.org /ISSN:1943-8141/AJTR0025639

Original Article

Effects of combined delivery of extremely low frequency electromagnetic field and magnetic Fe_3O_4 nanoparticles on hepatic cell lines

Huixiang Ju, Yubao Cui, Zhiqiang Chen, Qinping Fu, Mingzhong Sun, Ying Zhou

Department of Clinical Laboratory, Affiliated Yancheng Hospital,School of Medicine, Southeast University, Yancheng 224001, Jiangsu Province, P. R. China

Received February 5, 2016; Accepted March 6, 2016; Epub April 15, 2016; Published April 30, 2016

Abstract: Magnetic Fe_3O_4 nanoparticles (MNPs) have shown promise as drug carriers for treating lung and liver tumors in vivo. However, little is known about the combined delivery of these MNPs with a second approach, extremely low frequency electro-magnetic field (ELFF) exposure, which has been shown to have value for in vitro treatment of tumor cells. Here, ELFF and MNPs were combined to treat healthy (HL-7702) and cancerous (Bel-7402, HepG2) hepatic cells lines to explore the potential therapeutic effects, bio-mechanisms, and potential toxicity of a combined drug-free treatment in vitro. Flow cytometry for anti-AFP (alpha fetal protein) antibody, which coated the MNPs, indicated that the combined treatment induced Bel-7402 and HepG2 hepatoma cells lines into early apoptosis, without significant effects on healthy hepatic cells. This effect appeared to be mediated through cellular membrane ion metabolism. The presence of AFP-loaded MNPs strengthened the effects of ELFF on tumor cells, inducing a higher frequency of early apoptosis, while having minimal toxic effects on healthy HL-7702 cells. Western blotting revealed that the apoptosis-triggering BCL proteins were up regulated in hepatoma cells compared to healthy cells. Flow cytometry and patch-clamp studies revealed that this resulted from a higher MNP uptake ratio and greater cellular membrane ion exchange current in tumor cells compared to HL-7702 cells. Further, patch-clamp results showed that combining MNPs with ELFF treatment induces cells into early apoptosis through an ion metabolism disturbance in cells, similar to ELFF treatment. In brief, the combination of ELFF and MNPs had beneficial effects on tumor cells without significant toxicity on healthy cells, and these effects were associated with cellular MNP uptake.

Keywords: Hepatic cell lines, early apoptosis, extremely low frequency altering electro-magnetic field, magnetic nano Fe_3O_4 particles loading AFP-MA, alpha fetal protein mono-clonal antibody

Introduction

Magnetic nano particles have been used as a drug carrier for targeted treatment of tumors, with drug release guided by an external static magnetic field. This approach has the potential to reduce the therapeutic drug dosages, resulting in lower toxicity and fewer adverse effects [1]. Magnetic Fe oxide particles, particularly magnetic nano Fe_2O_3 and Fe_3O_4 particles, are used widely in medicine, for example to treat lung and liver cancers [1]. Their super-paramagnetic property and small diameter allow these particles to more easily reach deep tumor foci under static magnetic field guidance [2, 3]. Extremely low frequency electro-magnetic field (ELFF) has been used in physical therapy to accelerate the healing process of patients [4]. Additionally, ELFF exposure has been shown to induce early apoptosis in liver and lung tumor cells in vitro [5]. However, ELFF physical chemistry properties have restricted its application to cancer therapy in vivo due to its low energy to penetrate through living tissues [5-8]. Research is scarce on the combined effects and mechanisms of action of ELFF and magnetic nano Fe_3O_4 particles (MNPs) on tumor cells.

To begin to understand the biological effects of combined MNPs and ELFF in tumor cells, in the current study MNPs loaded with alpha fetal protein monoclonal antibody (AFP-MA) were combined with ELFF to treat three hepatic cells lines: HepG2 and Bel-7402 hepatoma cells

lines. MNP uptake by the cellular membrane and cellular apoptosis were detected by flow-cytometer, and Western-blot and patch-clamp studies were used to investigate the possible molecular mechanisms of the combined treatment on these cells.

Materials and methods

Materials

RPMI 1640 culture medium, Trizol reagent, fetal bovine serum (FBS), phosphate-buffered saline (PBS), and dimethyl sulfoxide (DMSO) were purchased from Gibco (USA). Anti-Bcl-2 and anti-Bax mouse resource monoclonal antibodies were from Santa Cruz Biotechnology (USA). Analytical pure $FeSO_4 \cdot 6H_2O$, $FeCl_3 \cdot 7H_2O$, NaOH, glycerin, and alcohol were obtained from Nanjing Chemicals Company (China). Bel-7402 and HepG2 hepatoma cells lines and HL-7702 cell lines were purchased from Institute of Materia Medica, Chinese Academy of Medical Science. Cells were routinely examined and found to be free of mycoplasma contamination, and were grown in RPMI 1640 medium supplemented with 10% FBS, 100 U/mL penicillin, and 100 μg/mL streptomycin at 37°C in a humidified atmosphere of 5% CO_2 and 95% air.

ELFF regenerator comprised a frequency converter (operating region 0.01 Hz to 199 Hz, the lowest step 0.01 Hz, Wangcheng electronic cooperation, Nanjing, China), electric potential transformer (operating region 12 V to 380 V, Fuji electric company, Shanghai, China), actuating coil (1 mm diameter copper lines, inner diameter 10 cm and outer diameter 14 cm, height 22 cm, 240 windings), regulating consistence (resistance 12 Ω, 70°C highest working temperature and current 15 A), and current source. The magnetic field was generated by copper coils. Anti-magnetic materials (polyvinyl dichloride) coated the copper to avoid the inter influences between different copper lines. The generating power was normal 50 Hz three-phase civil electric power.

Nano particle preparation and characterization

Flux co-precipitation method was utilized to prepare Fe_3O_4 particles from the reaction of $FeSO_4$, $FeCl_3$, and NaOH. The ratio of $FeSO_4$: $FeCl_3$ was 5:7 (content ratio). Briefly, $FeSO_4$ and $FeCl_3$ were dissolved in water and glycerin (9:1 mass ratio). The concentration of the Fe ion was maintained below 0.2 mol/L. 0.35 mol/L NaOH were added to a beaker with stirring (1500 rpm). The pH was detected in real time; at pH 7.4, the reaction was terminated and the solution was left for 1 h to allow particle curing. The solution was filtered by 1 T static magnetic field. Particles were washed for depolarization and organic matter clearance with pure water. Hydration particles were prepared and dried for 3 h. Finally, Fe_3O_4 particles were prepared. The reaction equation is shown in formula (1)

$$FeCl_3+2FeSO_4+8NaOH \rightarrow Fe_3O_4 \downarrow +4H_2O \quad (1)$$

Particles were 24 h and characterized by Transmission Electron Microscope (TEM) and X-ray Diffraction (XRD).

Particle ζ potential in culture medium

Particle surface potential for absorbing ions in culture medium was measured by the ζ potential method. Briefly, 5 mg of particles were suspended in 50 mL culture medium with 1500 Hz sonic exposure. The ζ potential of particles was measured by cupulate open micro electrophoretic apparatus (JS94, Shanhai Jiecheng Cooperation). The entire system was exposed to ELFF to determine the potential changes caused by ELFF, with the medium pH varied from 6.5 to 7.5 (modified by HCl or NaOH) to simulate the changes in cell culture conditions.

Particle co-culturing with cells and ELFF exposure

Particles (500 μg/mL) were added to cell culture flasks and washed by PBS twice, until the cells were re-suspended for subsequent detection. Cells were washed by PBS twice in room temperature to wash out the particles gathering on the flask bottom and suspended in culture medium to avoid influencing the following detection.

Cells were exposed to ELFF by 100 Hz, 0.7 mT magnetic inducing intensity generated by working coils with 11.5 A electric current and potential 240 V in cell culture flasks. The cell culture flasks were exposed to 100 Hz ELFF in working coils 2 cm from the apex. Cells were placed in

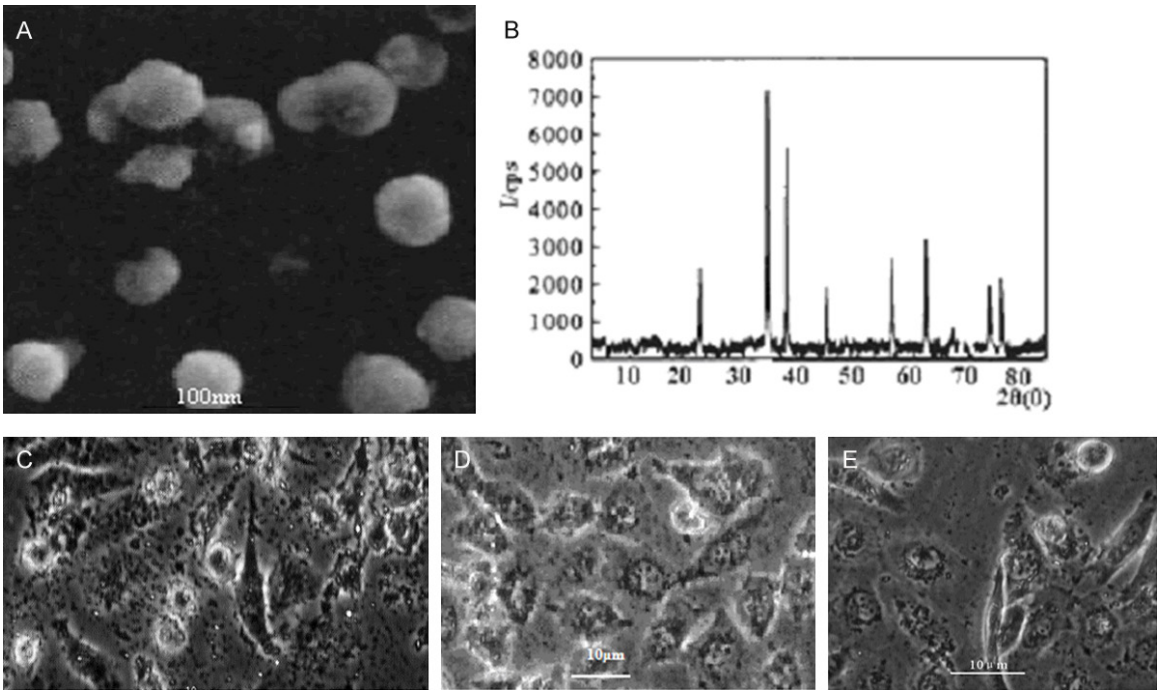

Figure 1. Co-culture of Bel-7402, HepG2, and HL-7702 cells with 40 nm magnetic Fe_3O_4 particles as assessed by transmission electron microscopy (TEM) and x-ray diffraction (XRD). (A) particles modified as 10000 TEM; (B) particles XRD; (C) HepG2 cells treated with MNPs combined with ELFF; (D) Bel-7402 cells treated with MNPs combined with ELFF; (E) HL-7702 cells treated with MNPs combined with ELFF.

an incubator after exposure for proliferation and detection. After each exposure, cells were digested by trypsin with 10% EDTA to generate a suspension for deep detection.

Particle uptake on cells

Particle uptake on cells was detected by FACstation following previous methods [8, 9]. Cells were treated with 500 μg/mL Fe_3O_4 particles loaded with anti-AFP monoclonal antibody for pre-determined periods, then trypsinized and re-suspended in medium. The amounts of particles taken up by the cells were analy-zed using a flow cytometer (FACstation) at 488 nm. The side scatter (SS) height was used to measure the proportion of cells taking up particles.

Cell apoptosis and associated protein expression

Cell apoptosis was detected on FACstation using experimental kits for apoptosis detection. Adherent cells (1×10^6) were washed twice with PBS (containing 2% FBS), trypsinized, and re-suspended in 200 μL of PBS supplemented with FBS. Cells were incubated with 30 μg/mL fluorescein isothiocyanate (FITC), ANNEXIN-V, and 20 μL/mL propidium iodide (PI) in the dark for 30 min at 37°C and maintained on ice until analysis. Fluorescence intensities of ANNEXIN-V-FITC and PI were determined by FACstation. Control cells were used throughout each assay. At least 10000 cells per sample were analyzed and measurements were performed in triplicate. The total protein was separated on 17% polyacrylamide gels, analyzed, and transferred to Immobilon P membranes. Blocking was performed by incubating the PVDF membranes with 5% (w/v) non-fat dry milk in Tris-buffer saline (TBS), pH 7.4, for 1 h at room temperature and under continuous agitation. The membranes were then incubated with anti-BCL-2 or anti-BAX (1:400 and 1:200, respectively) in 5% non-fat dry milk in TBS, 0.05% Tween-20 (TBS-T) for 3 h at room temperature under continuous agitation. Horseradish peroxidase-conjugated goat anti-rabbit IgG at a dilution of 1:2500 in 3% nonfat dry milk in TBS-T was incubated with membranes for 1.5 h at room temperature under continuous agitation. Detection of immunoreactive bands was performed by diaminobenzidine (DAB-Sigma, St. Louis, MO, USA) on the

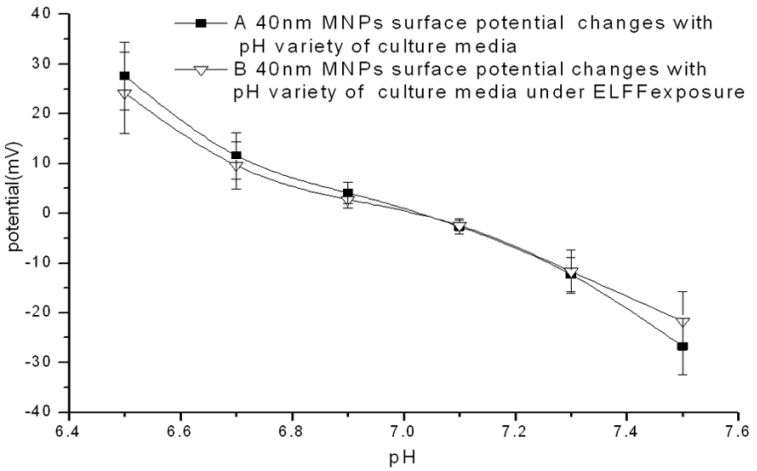

Figure 2. Changes in MNP surface ζ potential with pH of culture media. All data were measured at 298 K temperature.

manufacturer's instructions. The pictures were quantitated using the ImagePC image analysis software (Scion Corporation, Frederick, MD, USA).

Cellular membrane electric inflow current detection

Patch-clamp experiments were conducted at room temperature in the whole cell configuration using an Axopatch 200B patch-clamp amplifier and associated standard equipment (Axon Instruments, Foster City, CA). Cells were continuously super-fused with bath solution containing 140 mmol/L NaCl, 4 mmol/L CsCl, 2 mmol/L $CaCl_2$, 2 mmol/L $MgCl_2$, and 10 mmol/L HEPES, adjusted to pH 7.4 with NaOH. Patch pipettes were pulled from borosilicate glass and typically had a resistance of 1-3 mmol/L when filled with the standard pipette solution containing 40 mmol/L CsCl, 85 mmol/L Cs glutamate, and 10 mmol/L EGTA-Na, 10 mmol/L HEPES, adjusted to pH 7.2 with NaOH. Series resistance did not exceed 3 mol/L and was 75-85% compensated. Currents obtained were filtered at 2 kHz, collected, and analyzed using Clampex 9.0 Software.

Statistical analysis

Each experiment was performed at least three times, and the results are expressed as mean values ± S.D. (n=2-6). The Student's t-test was used to determine the significance of differences between the mean values obtained for the two cell lines. Otherwise, the various treatments were analyzed using one-way analysis of variance (ANOVA) followed by either Dunnett or Bonferroni multiple comparison test. $P<0.05$ was considered as statistically significant.

Results

Particle characterization and co-culture with cells

Analysis of the nanoparticles by TEM (**Figure 1A**) showed particles were an irregular ball shape, and the mean diameters were about 40 nm. XRD analysis (**Figure 1B**) revealed some Fe and O element-specific peaks, and the value of Fe:O was nearly 0.74. Therefore, the particles should be Fe_3O_4 particles (MNPs). MNPs dispersed in culture medium uniformly around the three kinds of cells (**Figure 1D-F**). MNPs ζ potential changing curves in culture medium (**Figure 2**, line A) revealed MNPs were electric-negative after culture in medium at pH 7.0, illustrating that MNPs should absorb some cations on the surface due to the small diameter and huge specific area effects. Further, the addition of ELFF exposure did not influence the MNPs ζ potential in culture medium (**Figure 2**, line B).

MNP uptake on cells

MNPs could be taken up by cells after co-culturing (**Figure 3**). The three kinds of hepatic cell lines took up some MNPs on their membrane surface. The percentages of cells taking up MNPs were 35.6±8.3%, 34.5±6.2%, and 4.2±5.6% corresponding to Bel-7402, HepG2, respectively. MNP uptake was significantly more common among tumor cells (Bel-7402 and HepG2 lines) compared to healthy hepatic HL-7702 cells ($P<0.05$). After ELFF exposure, a small quantity of MNPs were removed from the cellular membrane into the culture medium; the percentage decreases in bound MNPs for Bel-7402, HepG2, and HL-7702 cells were 7.4±2.1%, 6.9±1.8%, and 1.3±2.7%, respectively.

Cellular apoptosis

To determine the effect of MNP uptake and/or ELFF treatment on hepatic cell lines, early

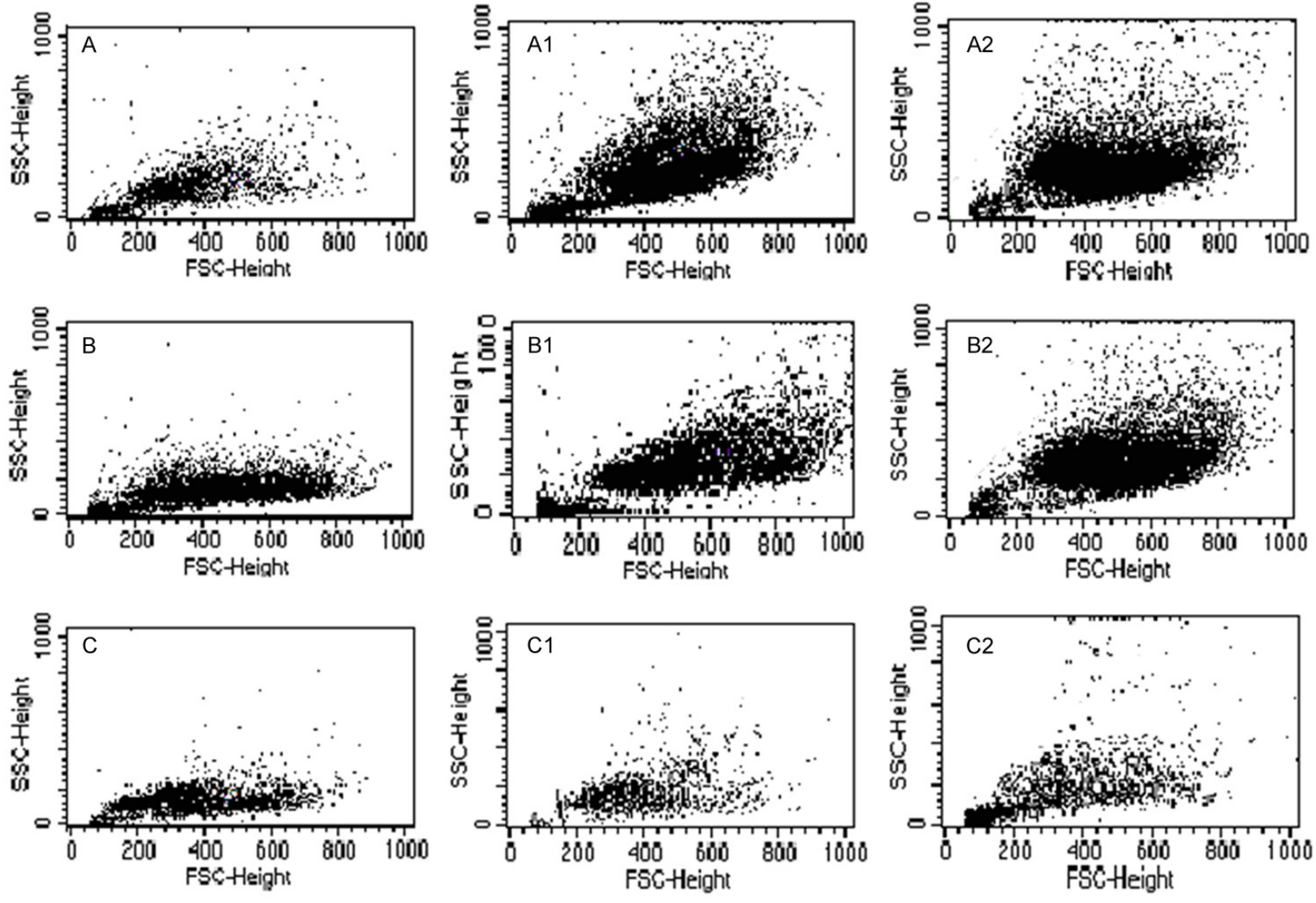

Figure 3. MNP uptake in three hepatic cell lines determined by flow cytometry for the AFP coating. (A) Bel-7402 cells treated or un-treated by MNPs (A1) and ELFF (A2); (B) HepG2 cells treated or un-treated by MNPs (B1) and ELFF (B2); (C) HL-7702 cells treated or un-treated by MNPs (C1) and ELFF (C2).

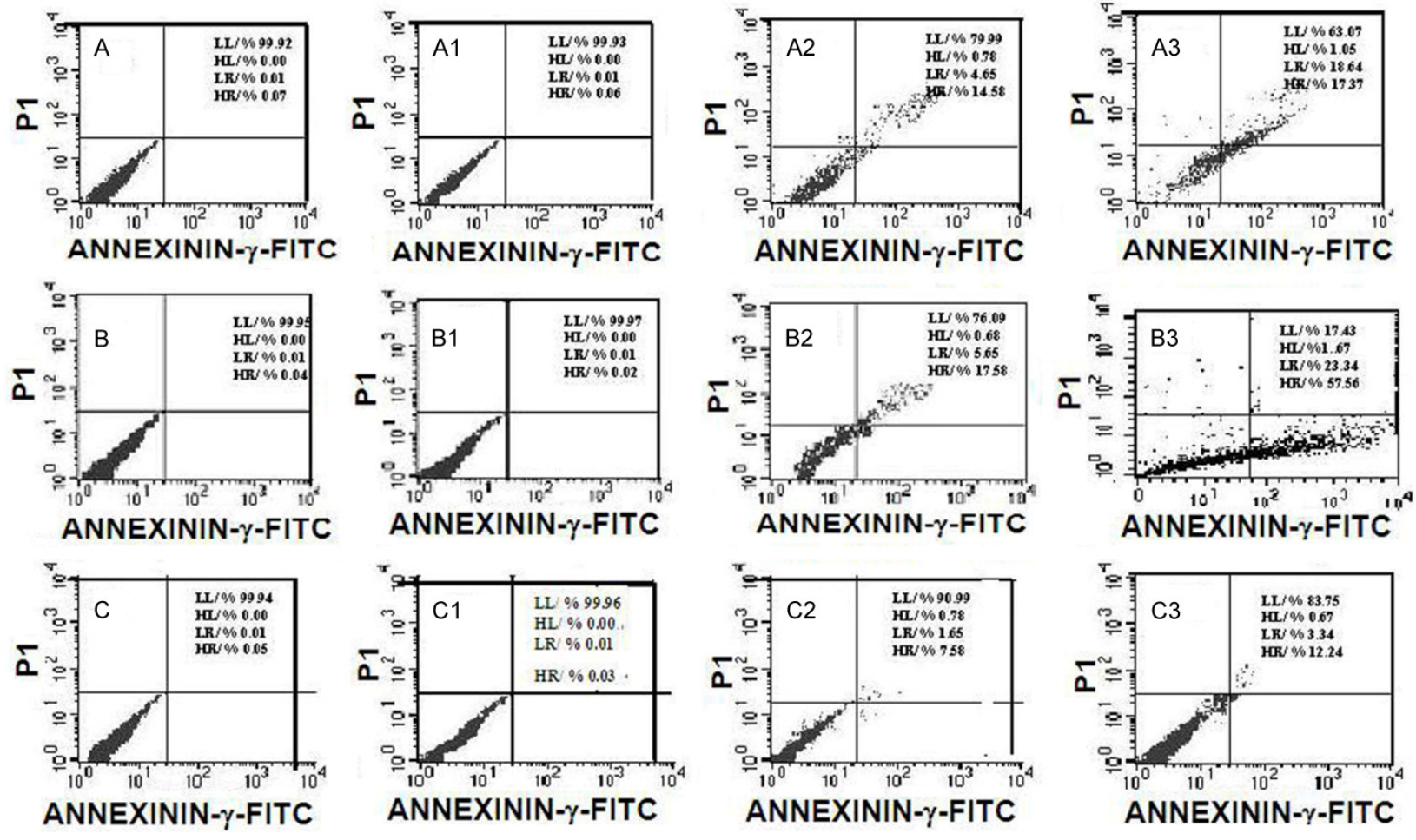

Figure 4. Early apoptosis and necrosis of Bel-7402 cells, HepG2, and HL-7702 cells treated with MNPs and ELFF. (A) Bel-7402 cells sham control; (A1) Bel-7402 uptake of MNPs; (A2) Bel-7402 exposed to ELFF; (A3) Bel-7402 uptake of MNPs after exposure to ELFF. (B) HepG2 cells control; (B1) HepG2 uptake of MNPs; (B2) HepG2 exposed to ELFF; (B3) HepG2 uptake MNPs after exposure to ELFF. (C) HL-7702 cells control; (C1) HL-7702 uptake of MNPs; (C2) HL-7702 exposed to ELFF; (C3), HL-7702 uptake of MNPs after exposure to ELFF.

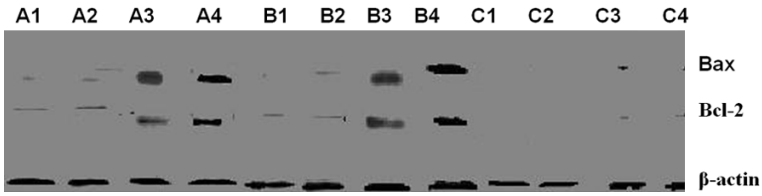

Figure 5. Early apoptosis-associated protein expression of cells treated with MNPs and/or ELFF. A1, Bel-7402 sham control cells; A2, MNP-treated Bel-7402 cells; A3, ELFF-treated Bel-7402 cells; A4 MNPs combined with ELFF in Bel-7402 cells. B1, HepG2 sham control; B2, MNP-treated HepG2 cells; B3, ELFF-treated HepG2 cells; B4, MNPs combined with ELFF in treating HepG2 cells. C1, HL-7702 cells sham control; C2, MNP-treated HL-7702 cells; C3, ELFF-treated HL-7702 cells; C4, MNPs combined with ELFF in treating HL-7702 cells.

apoptosis was measured by flow cytometry for BCL-2 and BAX, two proteins involved in apoptosis signaling. **Figure 4** shows the early apoptosis of cells treated with MNPs and ELFF, compared to those without ELFF exposure. In cell lines treated with MNPs only, apoptosis was not increased (**Figure 4A1**, **B1**, **C1**). ELFF exposure alone could induce some cells into early apoptosis, about 7.26±3.8% for HepG2 cells and 4.65±1.2% for Bel-7402 cells (**Figure 4A2**, **B2**) and just 1.05±0.5% of HL-7702 cells (**Figure 4C2**). The differences between cancer cell lines and the control were statistically significant ($P<0.05$), which could suggest tumor cells are more susceptible to ELFF exposure. The combined MNPs and ELFF treatment exacerbated the induction of apoptosis in the cells (**Figure 4A3**, **B3**, **C3**); the percentages of apoptotic cells were 22.34±6.2%, 18.64±5.7%, and 3.34±1.5%, respectively. Again, apoptosis was significantly more frequent among tumor cells than healthy hepatic cells ($P<0.05$). The difference between the two tumor lines, however, was not statistically significant ($P>0.05$).

Early apoptosis-associated protein expression

Consistent with the findings by flow cytometry, MNP treatment alone did not influence the level of BCL-2 and BAX proteins detected in the cell lines by immunoblotting (**Figure 5**). However, ELFF exposure alone did result in upregulated BCL-2 protein levels in all three cell lines. The BCL-2: BAX ratio in Bel-7402 cells was 0.93 and in HepG2 cells was 0.91, compared to 0.99 in HL-7702 cells; these differences were not statistically significant. When MNP and ELFF treatment were combined, the presence of MNPs strengthened the effects of ELFF on protein levels in tumor cells: the BCL-2/BAX ration was 0.84 in Bel-7402 cells and 0.82 in HepG2 cells, which were significantly lower than the ration in HL-7702 cells (0.98; $P<0.05$).

Cellular membrane electro-exchange current

Patch-clamp experiments indicated that ELFF exposure alone and MNPs combined with ELFF treatment on cells influenced cellular membrane ion electro-exchanges (**Figure 6**). The anion inflow exchanging electro-current of tumor cells was significantly higher than that of healthy hepatic cells. The initial inflow currents of Bel-7402, HepG2, and HL-7702 cells were 2.1, 2.2, and 1.2 pA, respectively, at pH7.2 and 20 mV. ELFF exposure reduced cell anion inflow currents, especially for tumor cells: the 42.9% and 40.0% inflow anion current of Bel-7402 and HepG2 cells, respectively were significantly higher than for the HL-7702 cells (25.0%). Further, the presence of MNPs strengthened the reduction of cell inflow current over that of ELFF alone; the percent reduction of current in Bel-7402, HepG2, and HL-7702 cells was 57.1%, 54.5%, 25.7%, respectively. The difference between tumor cells and control cells was significant ($P<0.05$). However, the reduction of current in HL-7702 cells treated by MNPs combined with ELFF versus ELFF alone was not significantly different ($P>0.05$).

Discussion

Ions play important roles in cell proliferation and survival. For example, Ca^{2+} is critical for organelle membrane skeletal structure, and PO_4^{3-} is needed in cellular membrane and mitochondrial membrane synthesis. Ion metabolism disturbances can activate early apoptosis associated with signal channels and induce cells, especially tumor cells with faster ion metabolism ratio or higher inflow/outflow ion electric current, into early apoptosis [10-14]. ELFF produces magnetic field effects on cells that could influence ion metabolism by affecting ion movements. The generally accepted theory about cellular ion metabolism is that ion

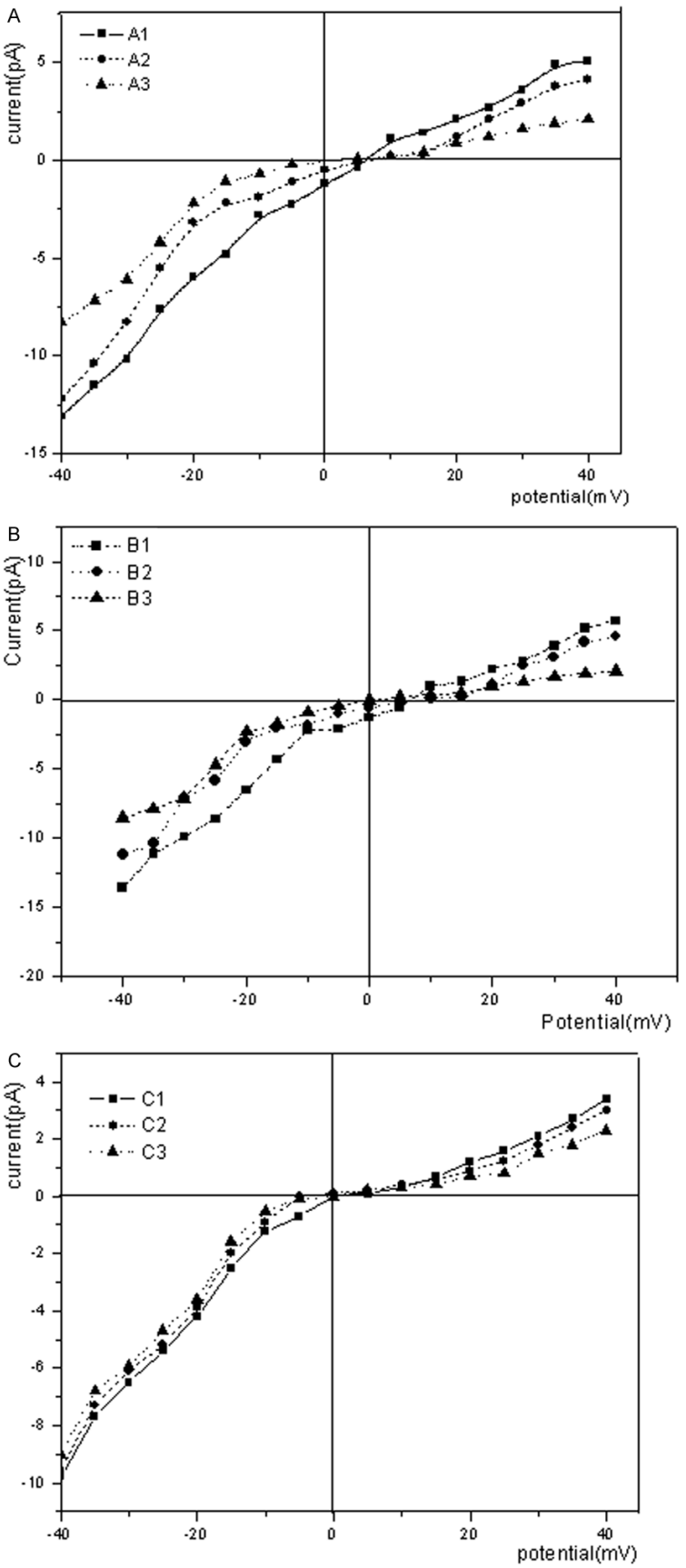

Figure 6. The electric outflow current of cell membranes with or without the presence ELFF. (A) current-voltage relationships derived from the above corresponding recordings of Bel-7402 cells; (B) current-voltage relationships derived from the above corresponding recordings of HepG2 cells; (C) current-voltage relationships derived from the above corresponding recordings of HL-7702 cells. A1, B1, C1 represent sham controls of their corresponding cell lines. A2, B2, C2 represent ELFF treatment alone of corresponding cell lines. A3, B3, C3 represent MNP plus ELFF treatment of the corresponding cell lines.

transformation on cell membranes is based on transforming proteins in the cellular double chlorine layers, and the transforming protein acts as ion channels or ion signal channels [15, 16].

In this study, MNPs were dispersed in the culture media evenly throughout the culture and experimental procedures, without obvious aggregations (**Figure 1C-E**). The uptake of MNPs was more common among tumor cells than healthy cells. ELFF was utilized to expose cells for investigating whether MNPs could be removed from the cellular membrane. Small amounts of MNPs were removed from both kinds of tumor cells; however, the removal of MNPs was significantly lower for HL-7702 than tumor cells after ELFF exposure. This phenomenon hinted that tumor cells possess more constraining forces to MNPs, potentially due to a higher positive electric potential and larger membrane surface exposed to MNPs on tumor cells. MNP electric ζ potential was negative in culture medium, while all three kinds of hepatic cells

were electropositive (**Figure 6A-C**). Both kinds of tumor cells had a higher surface positive potential than HL-7702 cells.

Interestingly, the tumor cells also displayed greater early apoptosis rates than control cells when treated by ELFF alone. BCL-2 protein was upregulated following ELFF exposure (**Figure 5**), but more so in tumor cells than in healthy cells. The BCL protein family is associated with cellular ion metabolism and can be highly expressed when ion metabolism is disturbed by external factors like ion movement direction and blocked ion channels [17, 18]. Cell ion disturbance was confirmed by patch-clamp experiments. After ELFF exposure, the three kinds of hepatic cells had reduced cation inflow/outflow currents, and the reduction was greater for tumor cells than healthy cells.

The larger surface area of tumor cells could offer cells more area exposed to ELFF and MNPs. Higher ion exchange currents could be interpreted as faster ion movement or electric current through the cell membrane. As classical electro-magnetic field theory described, a higher electric current or faster ion movement could generate higher magnetic field [19, 20]; thus, the magnetic field interaction force between ELFF and tumor cells was higher than the interaction force between ELFF and healthy hepatic cells, at the same ELFF exposure dose. Additionally, MNP electric-negative potential could enhance the treatment effects of ELFF on cellular ion disturbance.

Furthermore, MNPs combined with ELFF treatment induced more tumor cells into early apoptosis than in cells treated by ELFF alone or in HL-7702 cells. This likely results from more tumor cells taking up MNPs on the surface, and the larger surface area of tumor cells and higher ion exchanging current. MNPs, as superparamagnetic and small-diameter particles, could conduct external magnetic fields to affect cells after their dispersal in culture medium, and strengthen the effect of ELFF by influencing ion metabolism.

In summary, the combination of ELFF and MNPs produced greater apoptosis of hepatoma cell lines than of healthy control hepatic cells. Further, western blot and patch clamp experiments showed the combined treatment of ELFF and MNPs on cells should be partially based on the ion metabolism disturbance of the cellular membrane due to ELFF magnetic field effects and MNPs strengthening ELFF effects on tumor cells. Therefore, the combination treatment had beneficial effects on tumor cells without significant toxicity on healthy cells, and these effects were associated with cellular MNP uptake.

Acknowledgements

This work was funded by Study Project of Healthy Department of Jiangsu province (No: H201257) and Six kinds of the Talent Peak Project of Jiangsu Province (No: 2011-WSN-019).

Disclosure of conflict of interest

None.

Address correspondence to: Huixiang Ju, Department of Clinical Laboratory, Affiliated Yancheng Hospital, School of Medicine, Southeast University, No. 75 at Juchang Road, Yancheng 224001, Jiangsu Province, P. R. China. Tel: +8651581608616; E-mail: huixiangjuyc@hotmail.com

References

[1] Long NV, Thi CM, Yong Y, Cao Y, Wu H, Nogami M. Synthesis and characterization of Fe-based metal and oxide based nanoparticles: discoveries and research highlights of potential applications in biology and medicine. Recent Pat Nanotechnol 2014; 8: 52-61.

[2] Dastjerdi R, Montazer M. A review on the application of inorganic nano-structured materials in the modification of textiles: focus on anti-microbial properties. Colloids Surf B Biointerfaces 2010; 79: 5-18.

[3] Vajo JJ. Influence of nano-confinement on the thermodynamics and dehydrogenation kinetics of metal hydrides. Curren Opit in Sol Stat & Mat Sci 2011; 15: 52-61.

[4] Costin GE, Birlea SA, Norris DA. Trends in wound repair: cellular and molecular basis of regenerative therapy using electromagnetic fields. Curr Mol Med 2012; 12:14-26.

[5] Stam R. Electromagnetic fields and the blood–brain barrier. Brain Res Rev 2010; 65: 80-97.

[6] Johansson O. Disturbance of the immune system by electromagnetic fields-A potentially underlying cause for cellular damage and tissue repair reduction which could lead to disease and impairment. Pathophy 2009; 16: 157-177.

[7] Genuis SJ. Fielding a current idea: exploring the public health impact of electromagnetic radiation. Public Health 2008; 122: 113-124.

[8] Hiroshi S, Tatsushi T, Yuko I. Simple and easy method to evaluate uptake potential of nanoparticles in mammalian cells using a flow cytometric light scatter analysis. Environ Sci Technol 2007; 41: 3018-3024.

[9] Coester C, Nayyar P, Samuel J. In vitro uptake of gelatin nanoparticles by murine dendritic cells and their intracellular localization. Eur J Pharm Biopharm 2006; 62: 306-314.

[10] Jonas EA. Contributions of Bcl-xL to acute and long term changes in bioenergetics during neuronal plasticity. Biochim Biophys Acta 2014; 1842: 1168-78.

[11] Mangwani N, Shukla SK, Rao TS, Das S. Calcium-mediated modulation of Pseudomonas mendocina NR802 biofilm influences the phenanthrene degradation. Colloids Surf B Biointerfaces 2014; 114: 301-9.

[12] Vostrikov VV, Mote KR, Verardi R, Veglia G. Structural Dynamics and Topology of Phosphorylated Phospholamban Homopentamer Reveal Its Role in the Regulation of Calcium Transport. Structure 2013; 21: 2119-30.

[13] James AW, Nachiappan V. Phosphate transporter mediated lipid accumulation in Saccharomyces cere- visiae under phosphate starvation conditions. Biores Technol 2014; 151: 100-105.

[14] Hassan MA, Campbell P, Kondo T. The role of Ca^{2+} in ultrasound-elicited bioeffects: progress, perspectives and prospects. Drug Discov Today 2010; 15: 892-906.

[15] Hutcheson JD, Schlicher RK, Hicks HK, Prausnitz MR. Saving Cells from Ultrasound-Induced Apoptosis: Quantification of Cell Death and Uptake Following Sonication and Effects of Targeted Calcium Chelation. Ultrasound Med Biol 2010; 36: 1008-21.

[16] Le Y, Shuwen L. Autophagy contributes to modulating the cytotoxicities of Bcl-2homology domain-3 mimetics. Semin Cancer Bio Part B 2013; 23: 553-560.

[17] Takahashi H, Chen MC, Pham H, Matsuo Y, Ishiguro H, Reber HA, Takeyama H, Hines OJ, Eibl G. Simultaneous knock-down of Bcl-xL and Mcl-1 induces apoptosis through Bax activation in pancreatic cancer cells. Biochim et Biophy Act (BBA) - Molec Cell Res 2013; 1833: 2980-2987.

[18] Cole AJ, David AE, Wang J, Galbán CJ, Hill HL, Yang VC. Polyethylene glycol modified, cross-linked starch-coated iron oxide nanoparticles for enhanced magnetic tumor targeting. Biomaterials 2011; 32: 2183-2193.

[19] Sudeshna C, Barick KC, Bahadur D. Oxide and hybrid nanostructures for therapeutic applications. Advan Drug Del Revi 2011; 63: 1267-1281.

[20] Pilla AA. Electromagnetic fields instantaneously modulate nitric oxide signaling in challenged biological systems. Biochem Biophys Res Commun 2012; 426: 330-333.